International Journal of Heat and Technology
Vol. 42, No. 2, April, 2024, pp. 501-510
Journal homepage: http://iieta.org/journals/ijht

Numerical Study on Entropy Generation in a Horizontal Channel with Fins Using Hybrid Nanofluid

Moussa Khentoul*, Rachid Bessaïh

LEAP Laboratory, Department of Mechanical Engineering, Faculty of Technology Sciences, Constantine 1, Frères Mentouri University, Constantine 25000, Algeria

Corresponding Author Email: moussa.khentoul@umc.edu.dz

https://doi.org/10.18280/ijht.420216

Received: 12 January 2024
Revised: 19 March 2024
Accepted: 28 March 2024
Available online: 30 April 2024

Keywords:
entropy generation, finite volumes, fins, forced convection, hybrid nanofluid

ABSTRACT

This study involved performing a two-dimensional numerical analysis of forced convection in a horizontal channel, to cool fins mounted on heated channel walls, with the use of a laminar hybrid nanofluid. The finite volume approach, employing the SIMPLER algorithm, was used to solve the determining equations. The effect of fin height "hf", fin space "d" and nanoparticle volume fraction (ϕ) on the flow structure, entropy generation, and heat transfer enhancement are analyzed and discussed. The results were exposed in streamlines, isotherms, average Nusselt numbers, total and local entropy generation, thermal and friction, and the Bejan number. The results indicate that increasing the height of the fins leads to an improvement in heat transfer, but on the other hand, causes a notable elevation in entropy generation. The results further suggest that increasing the 'd' spacing (up to d=1.1) leads to a smooth and uniform passage of fluid between the fins, thereby reducing entropy generation. However, it also results in poor cooling of the fins.

1. INTRODUCTION

Forced convection heat transfer significantly impacts heat dissipation in electronic equipment and assumes a pivotal role in their design and performance. Adequate cooling plays a fundamental role in ensuring optimal efficiency and meeting the growing demands of modern electronic technology. Various cooling approaches have been suggested to ensure electronic equipment's stable and reliable operation. Among these methods, we find the use of expanded surfaces, the installation of fins, and the incorporation of nanoparticles into the base fluid. Many of the published works have been developed concerning heat transfer in channels that are directly related to our study; with different boundary conditions; among these studies, we find:

Ghaneifar et al. [1] executed a computational analysis on mixed convection involving nanofluid within a horizontally oriented channel. The channel features insulated walls and includes two centrally positioned heat sources. The results indicate that thermal conductivity, Reynolds and Richardson number, length/height ratio, and source separation distance considerably influence the thermal and flow field.

Naderifar et al. [2] numerically studied the flow pattern and heat transfer augmentation in a corrugated channel with a non-Newtonian nanofluid subjected to a constant thermal flux, with a fin. Moreover, the study demonstrates that including a fin induces a significant alteration in the temperature and flow fields, enhancing heat exchange.

Esfe et al. [3] investigated forced convection in a channel filled with the Al_2O_3-water nanofluid with walls considered isothermal. The numerical findings demonstrate enhanced heat transfer with the utilization of a nanofluid and also indicate that decreasing the nanoparticle diameter has the potential to improve heat transfer.

Mehreza and El Cafsi [4] conducted a numerical study of forced convection within a rectangular channel that contained ferrofluid subjected to a varying magnetic field created by four magnetic sources near radiators mounted on the bottom channel wall. The results show that elevating the Reynolds, magnetic numbers, and solid content ratio leads to enhanced heat exchange. The results also indicate an optimal position of the magnetic sources, which gives better thermal efficiency.

Hannachi et al. [5] studied the unstable forced convection of a non-Newtonian nanofluid to see the impact of the oscillating magnetic field in a channel containing heated permeable blocks. The findings show that entropy production and the heat exchange rate rise as ϕ decreases, alongside an increase in *Ri* and *Re* values. The results also indicate that, although sinusoidal heating contributes to heat transfer, it increases total entropy production.

A numerical study investigating the heat exchange and fluid flow within a horizontal rectangular porous channel utilizing a hybrid nanofluid was done by Jarray et al. [6]. Specific parameters such as the permeability (ε) of the porous medium, the *Da* and *Ri* number and ϕ to assess their impact on heat transfer rates and the flow field. Introducing hybrid nanoparticles into the water upgrades the heat transfer with different values of *Ri* and *Da* numbers.

Job et al. [7] researched the unsteady and incompressible flow in a horizontal channel of a hybrid nanofluid consisting of $MnZnFe_2O_4$/FeCrNbB. The top wall of the channel contains four porous fins. In contrast, the lower wall contains three

semi-circular radiators, where an electric wire generates an adjustable magnetic field magnetic field internally. the findings reveal that enhancing ϕ, the magnetic number, and the size of the heating element fins leads to increased convective heat transfer within the channel.

Ltaifa et al. [8] studied the mixed convection of a nanofluid, which is a combination of Al_2O_3 and water, flowing through a tilted rectangular microchannel, with the channel walls subjected to a regular thermal flux. The results indicate that increased inclination angles and higher volume fractions of Al_2O_3 contribute to an enhanced heat transfer rate.

Kalteh and Abedinzadeh [9] numerically examined flow structure and heat exchange within a microchannel occupied with a nanofluid. The channel experiences a consistent magnetic field, with the bottom wall maintained at a steady temperature, and the upper wall configured to be insulating. The findings reveal that an improvement in the heat transfer performance of the microchannel is observed with increased ϕ and *Re* numbers. The results additionally suggest that introducing a magnetic field elevates the friction factor, without significantly influencing heat transfer.

Heidary et al. [10] studied fluid and thermal flow analysis within a straight channel utilizing a nanofluid, incorporating a magnetic field into the flow structure, using a single-phase approach. Calculations show that a magnetic field and nanoparticles increase channel heat transfer.

Alqaed et al. [11] studied the entropy generation of a nanofluid in forced and natural convection inside a bidimensional closed compartment tilted and subjected to a magnetic field. Five heat sources positioned in the centre of the compartment create natural convection, and the movable upper wall causes forced convection. The results show that the effects of the angle of inclination of the closed container, the Bejan and Richardson numbers, have a considerable influence on the generation of entropy.

Zamzari et al. [12] analyzed the heat exchange and entropy generation associated with a pulsating airflow emerging from a downward-heated open cavity within a horizontal channel. The findings indicate that the entropy production and heat transfer are affected by both the amplitude and frequency of the pulsation, and this dependence is notably linked to the aspect ratio of the cavity and the Richardson number.

Hussain et al. [13] did a numerical investigation of mixed convection to explore the impact of parameters related to internal heat generation or absorption, porosity, and entropy generation. The results indicate a minimization in average heat transfer with the internal heat generation, while an increase is observed with the porosity. Moreover, the heat exchange and fluid friction-induced entropy production decreases in a magnetic field, while an augment is observed in the porosity parameter.

A numerical analysis is carried out to investigate heat transfer and entropy generation in a vertical channel with water-copper nanofluids is presented by Kahalerras et al. [14]. The channel is composed of a suitable wall cooled to a uniform thermal flux density and a left wall experiencing a sinusoidally varying thermal flux. The findings indicate an escalation in entropy generation and heat transfer as the solid volume fraction of the nanofluids decreases and with the increase in *Ri* and *Re*. The results also indicate that sinusoidal heating enhances heat transfer while simultaneously amplifying the overall entropy generation.

Kolsi et al. [15] numerically examined entropy and heat transfer generation inside a cubic enclosure packed with a water-Al_2O_3 nanofluid. The left wall is maintained at hot isothermal temperatures and the right wall is cold, and the other is assumed to be adiabatic. The results present that the Nu_{av}, S_{th}, S_{fr} and S_{total} increase with the increase in Ra number and ϕ, especially near the hot left sidewall.

Bhattacharyya et al. [16] analyzed the entropy generation and convective heat transfer in corrugated channels with walls at a uniform temperature. The findings indicated that the use of a corrugated channel gives a better heat transfer compared to a conventional circular channel. However, this improvement comes at the expense of increased frictional forces.

Abbaszadeh et al. [17] conducted a comprehensive study on entropy generation and heat transfer during forced convection within a parallel plate microchannel subjected to the impact of a magnetic field. The findings indicate that heat transfer and S_{total} increase with higher ϕ, and Ha and Re numbers. Conversely, as the Knudsen number rises, there is a notable decline in the S_{total}.

Vatanparast et al. [18] investigated forced convection to study entropy generation within a partially heated channel, employing semi-porous fins. The findings indicate that as the Reynolds number increases, there is a concurrent rise in Stotal, which attains a minimum value for a percentage of semi-porous fins (SFP=40). The fins' extension or broadening reveals an increased significance of S_{total}, a factor influenced by the thermal conductivity ratio.

Fersadou et al. [19] carried out a numerical investigation on entropy production in mixed convection with a nanofluid within a porous vertical channel. The findings indicated that using nanofluid, magnetic field and porous medium effectively enhances the heat transfer and elevates entropy generation.

Al-Rashed et al. [20] investigated the entropy generation and free convection heat transfer of heated fins in a cavity. Considering various Rayleigh number values, they identified the optimal fin number and length combination that maximizes heat transfer and entropy generation.

Ghachem et al. [21]’s study was carried out on natural convection and entropy production involving two configurations associated with the position of the baffle. The findings indicate that the baffle's placement significantly affects heat transfer and entropy production.

Alnaqi et al. [22] performed a numerical analysis to explore how the presence of a magnetic field, along with the influence of radiation, affects entropy generation, as well as the dynamics and thermal distribution within a diagonal square cavity using a fin located on one of the walls. The findings reveal that introducing nanoparticles to the base fluid and changes in the radiation parameter leads to an increase in entropy generation and the Nusselt number. Additionally, it was observed that the heat transfer rises with a decrease in the Ha number and an increase in the Rayleigh number.

A work on natural convection with a heat source in a cavity was presented by Shahi et al. [23], aiming to examine the entropy production of a nanofluid (Cu-water) for this considered problem. The findings indicate that positioning the heat source on the lower horizontal wall improves heat transfer and minimal entropy production.

Ahmed et al. [24] studied the hydrothermal performance and entropy production in a channel integrated with an oval rib. The results demonstrated that an elevate in rib height increases entropy production and heat transfer, across various Reynolds numbers.

The literature review reveals that most studies have highlighted the use of fins in a heated channel and their effect on flow characteristics and heat exchange within the channel.

In the complementary framework, we specifically focused on the impact of fin height and placement to achieve a more uniform flow and more efficient heat dissipation, which can reduce entropy generation associated with forced convection using a hybrid nanofluid.

2. PROBLEM MODELING

2.1 Problem description

Figure 1 shows a bidimensional horizontal channel with a length "L" and height "H", which must be cooled by Forced convection. The two-channel walls are subjected to a consistent temperature "T_h". The fins have a height "h_f" and a width "w", and are positioned on the walls with a space "S" between the fins in the same wall, and the offset between the fins of the lower and upper walls is "d". The hybrid nanofluid is used to cool the channel and introduced at a temperature T_0 and uniform speed U_0. The fluid is assumed to be Newtonian, laminar and incompressible. We consider a nanofluid to be in thermal equilibrium and have constant thermophysical properties. The thermodynamic properties of the base fluid (pure water) and the nanoparticle, at a fixed temperature of 25°C, are presented in Table 1 [25].

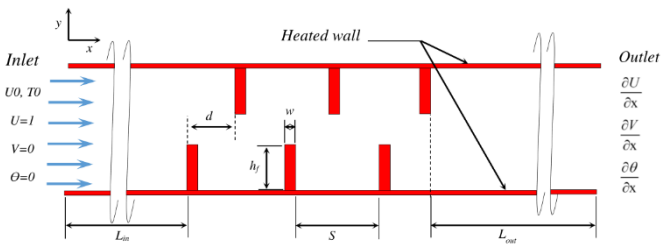

Figure 1. Geometry of the physical model

Table 1. Thermophysical properties of nanoparticles and water at 25°C

	ρ (kg/m^3)	C_p $(J/kg.K)$	k $(W/m.K)$	$\beta\times10^5$ $(1/K)$	$\alpha\times10^6$ (m^2/s)
Pure water	997.1	4179	0.613	21	0.147
Alumina (Al_2O_3)	3970	765	40	0.85	13.17
Copper	8933	385	401	1.67	116.31

2.2 Governing equations

The dimensionless equations governing two-dimensional, stationary, incompressible, Newtonian, and laminar flow are represented by the following equations:

Conservation of mass

$$\frac{\partial U_j}{\partial X_j} = 0 \tag{1}$$

Momentum equation

$$\frac{\partial U_j U_i}{\partial X_j} = -\frac{\partial P_i}{\partial X} + \frac{\mu_{nf}}{\rho_{nf}\nu_f}\frac{\nu^*}{\mathrm{Re}}\frac{\partial}{\partial X_j}\left(\frac{\partial U_i}{\partial X_j}\right) \tag{2}$$

Conservation of energy

$$\frac{\partial U_j \theta}{\partial X_j} = \frac{\alpha_{nf}}{\alpha_f}\frac{k^*}{\mathrm{Re\,Pr}}\frac{\partial}{\partial X_j}\left(\frac{\partial \theta}{\partial X_j}\right) \tag{3}$$

With: i=1, 2,

and: j=1, 2.

where k^* and ν^* are respectively the ratio of the conductivity and viscosity relative to the base fluid.

$$k^* = \begin{cases} = 400, & in\ the\ fin. \\ = 1, & in\ the\ fluid\ . \end{cases} \tag{4}$$

$$\nu^* = \begin{cases} \to \infty, & in\ the\ fin. \\ = 1, & in\ the\ fluid. \end{cases} \tag{5}$$

U_i, θ and P, are respectively, the dimensionless velocity components, temperature; and pressure.

In the above equations, the Reynolds and Prandtl numbers are presented as:

$$Re = \frac{U_0 H}{\nu_f} \text{ and } Pr = \frac{\nu_f}{\alpha_f} \tag{6}$$

The governing equations mentioned above are transformed into dimensionless forms using the following dimensionless parameters:

$$X = \frac{x}{H},\ Y = \frac{y}{H},\ U = \frac{u}{U_0},\ V = \frac{v}{U_0}$$
$$P = \frac{p}{\rho_{nf}U_0^2},\ \theta = \frac{T-T_0}{T_h-T_0} \tag{7}$$

Can be defined the nanofluid effective density as:

$$\rho_{nf} = (1-\phi)\rho_f + \phi_{Cu}\rho_{Cu} + \phi_{Al_2O_3}\rho_{Al_2O_3} \tag{8}$$

We can also determine the nanofluid thermal expansion coefficient $(\rho\beta)_{nf}$ as:

$$(\rho\beta)_{nf} = (1-\phi)(\rho\beta)_f + \phi_{Cu}(\rho\beta)_{Cu} + \phi_{Al_2O_3}(\rho\beta)_{Al_2O_3} \tag{9}$$

The determination of the heat capacitance of nanofluids involves:

$$(\rho C_P)_{nf} = (1-\phi)(\rho C_P)_f + \phi_{Cu}(\rho C_P)_{Cu} + \phi_{Al_2O_3}(\rho C_P)_{Al_2O_3} \tag{10}$$

where, ϕ_{Cu} and $\phi_{Al_2O_3}$ are the respective concentration volume of Cu and Al_2O_3; and $\phi = \phi_{Cu} + \phi_{Al_2O_3}$.

Maxwell–Garnetts [26] presented the nanofluid effective thermal conductivity as:

$$k_{nf} = \frac{k_s + 2k_f + 2\varphi\left(k_f - k_s\right)}{k_s + 2k_f + \varphi\left(k_f - k_s\right)} k_f \tag{11}$$

With:

$$k_s = \frac{\phi_{Cu} k_{Cu} + \phi_{Al_2O_3} k_{Al_2O_3}}{\phi} \tag{12}$$

Brikman [27] proposed the nanofluid effective dynamic viscosity as:

$$\mu_{nf} = \mu_f \left(1-\varphi\right)^{-2.5} \tag{13}$$

The thermal diffusivity of the nanofluid α_{nf} can be defined by:

$$\alpha_{nf} = \frac{k_{nf}}{\left(\rho c_p\right)_{nf}} \tag{14}$$

2.3 Boundary conditions

The following defines the boundary conditions in non-dimensional form:

At the channel entrance:

$$U = 1, \quad V = 0, \quad \theta = 0 \tag{15}$$

At the channel outlet:

$$\frac{\partial U}{\partial X} = 0, \quad \frac{\partial V}{\partial X} = 0, \quad \frac{\partial \theta}{\partial X} = 0 \tag{16}$$

At the bottom and top heated wall:

$$U = 0, \quad V = 0, \quad \theta = 1 \tag{17}$$

2.4 Local and average Nusselt numbers

Along the fins faces, we can present the local and average Nusselt number as:

$$Nu = -\frac{1}{\theta_b} \frac{k_{nf}}{k_f} \left(\frac{\partial \theta}{\partial n}\right)_{\substack{\text{exposed} \\ \text{surface}}} \tag{18}$$

The average Nusselt number Nu_{av} is:

$$Nu_{av} = \frac{1}{\left(w/H + 2h/H\right)} \int_{exposed\ surface} Nu dn \tag{19}$$

where, n and θ_b are respectively, the normal coordinate and the dimensionless temperature of the fin surfaces.

2.5 Entropy generation

We can determine the local and the total entropy generation as [23]:

$$S_{gen} = \frac{k_{nf}}{k_f}\left[\left(\frac{\partial \theta}{\partial X}\right)^2 + \left(\frac{\partial \theta}{\partial Y}\right)^2\right] + \chi\left[2\left(\frac{\partial U}{\partial X}\right)^2 + 2\left(\frac{\partial V}{\partial Y}\right)^2 + \left(\frac{\partial U}{\partial Y} + \frac{\partial V}{\partial X}\right)\right] \tag{20}$$

where,

$$\chi = \frac{\mu_{nf} T_0}{k_f}\left(\frac{U_0}{T_h - T_c}\right) \tag{21}$$

And

$$S_{total} = \int S_{gen} dV \tag{22}$$

3. NUMERICAL SOLUTION

3.1 Numerical method

The Fortran computational code with a control volume formulation was used to solve the dimensionless governing equations shown in Eqs. (1)-(3) as well as the boundary conditions in Eqs. (15)-(17). Velocities and pressure are calculated with the SIMPLER algorithm [28]; the diffusion and convection terms were treated by the centred difference scheme and the "upwind 2nd order" scheme. The discretized equations are then solved iteratively with a convergence criterion of 10^{-4} for continuity and 10^{-7} for momentum and energy, to give values for velocity, pressure and temperature at nodal points.

3.2 Grid independence study

Before commencing calculations, verifying that the solution remains unaffected by the mesh and that the numerical solution is accurate and reliable is necessary. In this study, we consider five different meshes with non-uniform sizes.

in the *x–y* coordinate directions, we considered five different meshes, 212×82, 322 ×82, 392×92, 452×102 and 602×122 nodes. As illustrated in Table 2, the variation of average Nusselt and the total entropy generation of the six fins was presented with the different meshes used with *Re*=100, *Pr*=0.72, ϕ=0 and 0.06.

According to Table 2, we observe that the values of the average Nusselt number and total entropy generation become insensitive to the number of nodes from the grid size of 452×102. Therefore, we opted for the mesh size of 452×102 nodes for all our calculations, to obtain qualitatively accurate results with minimal computation time.

Table 2. Grid independence study on the average Nusselt number

		212×82	322×82	392×92	452×102	602×122
ϕ=0	Nu_{av}	5.8915	5.5979	5.2944	5.2323	5.2461
	S_{total}	142.6990	142.7892	142.7408	142.7582	142.7594
ϕ=0.06	Nu_{av}	6.3236	5.9703	5.6229	5.6171	5.6150
	S_{total}	152.9723	154.2394	154.8198	154.8355	154.8374

3.3 Code validation

The calculation code was carefully reviewed and validated

with the numerical results of Pishkar and Ghasemi [29], to guarantee precision and robustness. A comparison has been conducted between the average Nusselt numbers (Table 3) of the two fins mounted on the heated lower wall of a horizontal channel cooled by Cu-water nanofluid under mixed convective, laminar conditions, with Reynolds numbers (Re=5, 100), and ϕ = 0.03.

According to Table 3, we observe a strong agreement among the results, which reassures us of the reliability of our calculation code.

Table 3. Validation of the current code with the numerical results from Pishkar and Ghasemi [29] for the average Nusselt numbers at Re=5, 10, 100, and ϕ=0.03

	ϕ	00	0.01	0.02	0.03
Re=5	Nu_{av} (Pishkar [29])	1.203	1.285	1.394	1.449
	Nu_{av} (Present study)	1.229	1.303	1.379	1.437
Re=100	Nu_{av} (Pishkar [29])	0.929	0.957	1.011	1.066
	Nu_{av} (Present study)	0.912	0.953	1.001	1.061

4. RESULTS

The results in this paper are presented for various parameters: fin height ($0.2 \le h_f \le 0.8$), space between the fins of the lower and upper walls ($0 \le d \le 1.6$), and concentration of solid nanoparticles ($0 \le \phi \le 0.6$).

Referring to Figure 1, the geometric parameters dimensionless by the height H are given as follows:

L/H=16, Li/H = 2, Le/H = 9.4, h_f/H =0.2 to 0.8, w/H = 0.2, S/H = 2.

4.1 Impact of fin height

We investigate the impact of dimensionless fin height on the flow field, thermal exchange, and entropy generation, with different fin author values h_f=0.2 to 0.8, S=2, d=0.9, Re=100 and ϕ=0 to 0.06.

Streamlines (top) and isotherms (bottom) show that increasing the fin size causes a substantial alteration in the flow and temperature distributions, which is presented in Figure 2. We observe that the fluid circulates freely for h_f = 0.2 due to the small size of the fins with small recirculation zones behind these fins.

The current lines show an undulating path of fluid between the lower and upper wall fins when increasing the height of the fins (h_f=0.4, 0.6, 0.8), and we also observe that the large size of the fins leads to the formation of large vortices behind the fins. We also notice an acceleration of the fluid when the passage section between the fins and the walls becomes smaller.

By consulting the same Figure 2, which presents the contours of the isotherms for different heights of the fins, we observe that the fluid starts with a low initial temperature and undergoes significant heating near the fins. It absorbs the heat emitted by the hot fins and transports it during its flow towards the outlet of the channel.

For h_f =0.2, the exchange surface between the fluid and the fins is small, and the liquid leaves without evacuating a large quantity of heat to the outside. This is why we observe that the isotherm lines parallel the heated wall, concentrated primarily around the fins, with a slight spreading within the channel.

On the contrary, for higher values of fin height (h_f=0.6 et 0.8 mm), Figure 2 shows the considerable heating of the fluid in the region located between the fins and that the isotherms occupy a significant part of the channel.

Also, the increase in the size of the fins increases the exchange area between the heated fins and the cool fluid. Also, the wavy path between the fins makes obtaining excellent interaction between the cool liquid and fin surfaces possible.

We also observed that the recirculation behind the fins has a significant impact and gives the fluid enough time to come into contact with the hot fins to transport a large amount of heat to obtain better cooling.

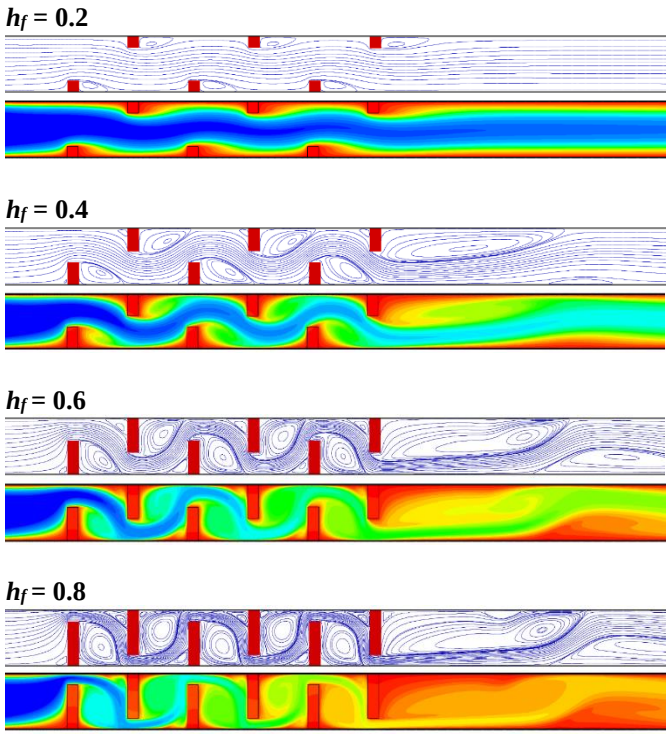

Figure 2. Isotherms (bottom) and streamlines (top) for a hybrid nanofluid (ϕ = 0.06) at various fin heights (hf), with Re=100

This is corroborated by Figure 3, which illustrates the variation in the fins' average Nusselt number (Nu_{av}) with their height for different values of the nanoparticle concentration in a hybrid nanofluid. As shown in Figure 3, Nu_{av} demonstrates an increase in the fin size.

Figure 3 also shows an increase in Nu_{av} corresponding to the concentration of nanoparticles. This result should be predictable since the presence of nanofluid nanoparticles enhances thermal conductivity and heat dissipation.

In the following, we will explore the influence of fin length (h_f =0.2, 0.4, 0.6, 0.8) on entropy generation (thermal, friction, total) and of the Bejan number for Re=100 and ϕ= 0 to 0.06.

Figure 4 illustrates the local entropy generation behaviour attributed to friction (top) and heat transfer (bottom) for various fin height values. Figure 4 clearly show that the obstacle compels the flow to deviate toward the walls, which causes large friction near the fins and wall, attributed to viscosity effects, which increases the generation of local entropy friction. The substantial influence of fin height on entropy generation is evident. Furthermore, an increase in fin height leads to an acceleration of nanofluid movement within this region. Consequently, the friction force increases,

contributing to a higher intensity of S_{fr}.

Figure 4 also shows high entropy generation values primarily arising from heat, resulting from pronounced temperature gradients. This effect is particularly notable in the heated walls and near the left corner of the fins. At the same time, the rest of the channel can be considered a relatively quiescent area in terms of entropy generation. Entropy generation escalates as the height fins rise, and elevated variations in velocity and temperature contribute to substantial thermal flux and increased entropy generation.

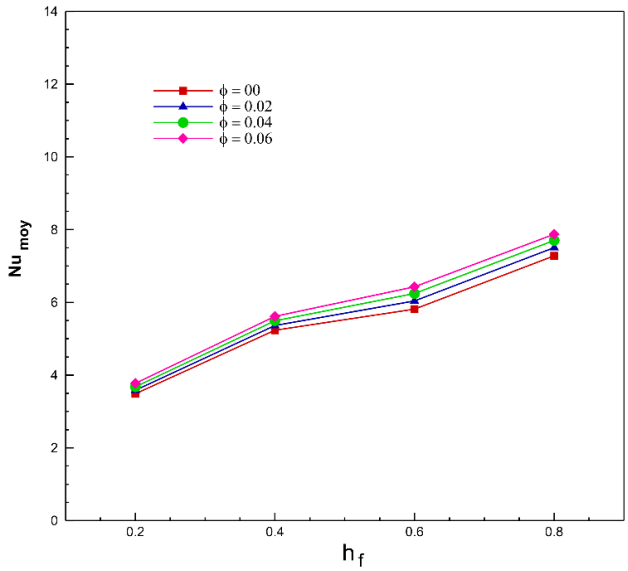

Figure 3. Influence of fin height (of hybrid nanofluid) on the average Nusselt number Nu_{av} across varying concentrations of solid nanoparticles, d=1.1 and Re=100

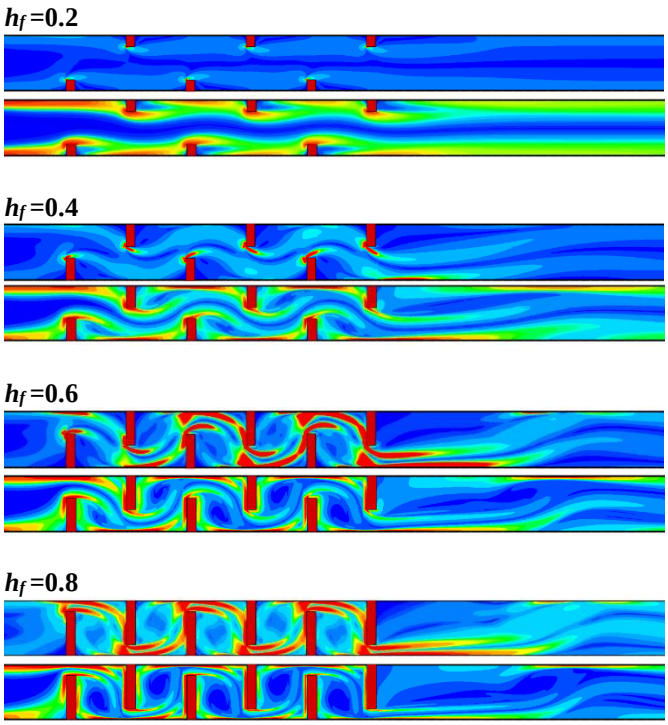

Figure 4. Variation in entropy generation resulting from friction (top) and heat transfer (bottom) for a hybrid nanofluid at different fin height values, Re=100 and ϕ=0.06

Figure 5 illustrates that the s_{total} was a function of fin height, considering the impact of nanoparticle concentration. The figure demonstrates a significant rise in total entropy generation as fin height increases, taking into account different nanoparticle volume rates. Additionally, it is noted that augmenting the ϕ enhances the conductivity and viscosity of the fluid. This results in an elevation in the S_{total} attributable to fluid friction and heat exchange.

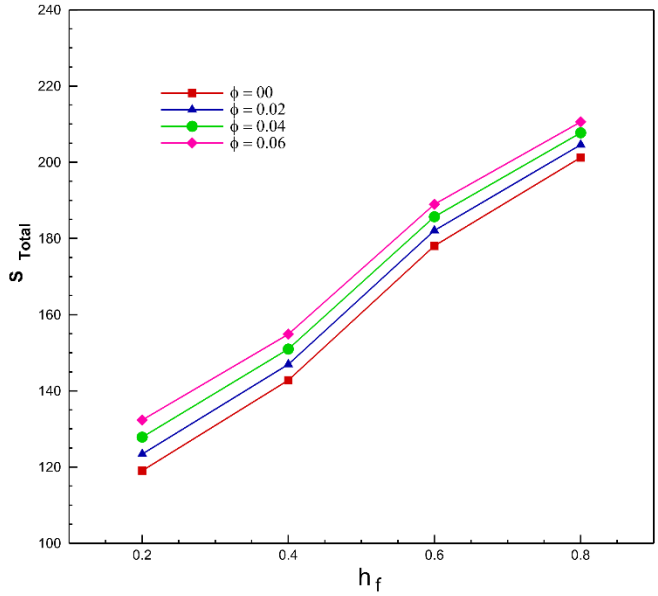

Figure 5. Influence of fin height on overall entropy generation across various volume concentrations of nanoparticles at Re=100 and d=1.1

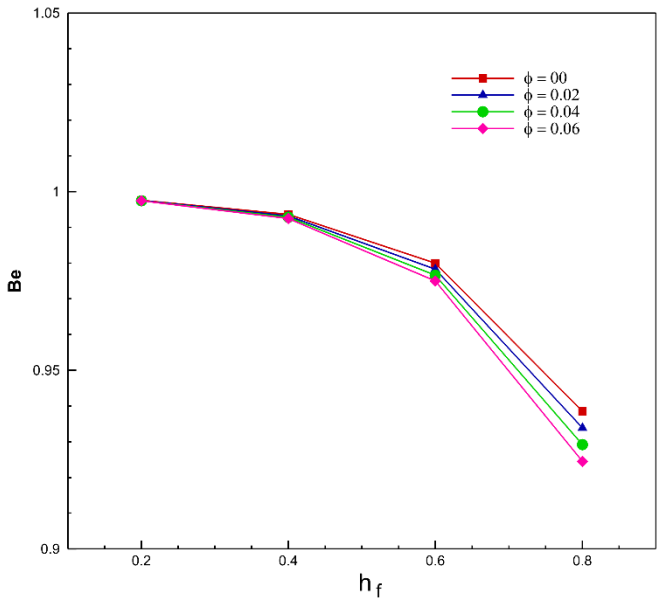

Figure 6. Effects of fin height on the Bejan number for different values of ϕ at Re=100 and d=1.1

Figure 6 illustrates the changes in the Bejan number (Be) across different fin heights and solid volume fractions, emphasizing the contributions of the two irreversibility modes to the overall value. Where it becomes apparent that S_{th} is prevailing. Figure 6 also indicates a noticeable reduction in the Be number with an increase in fin height. This decline can be ascribed to friction's heightened irreversibility compared to heat transfer. This phenomenon is likely attributed to the

increased intensity of viscous force resulting from the development of the movement of fluids due to the increase in the length of the fins, which also appears when the solid volume fraction is increased.

4.1 Effect of fin spacing

In this part, we examine the influence of the dimensionless space between the lower and upper wall fins "*d*" the entropy generation, heat transfer enhancement, and flow structure, with different values of space *d*=0 to 1.6, *Re*=100 and ϕ=0 to 0.06.

For important details of the effect of bottom and top wall fin separation on the overall flow characteristics and enhancing heat exchange, streamlines (upper) and isotherms (lower) for the hybrid nanofluid (ϕ=0.06) are depicted in Figure 7, for Reynolds number Re=100. These lines draw our attention that when the fins on the top and bottom walls are positioned opposite each other (*d*=0), it causes a congestion of the streamlines in the upstream corner, and also a narrowing of the section of the passage, which results in acceleration of the fluid. The fluid passage through the fins causes the development of large and vigorous vortices to form behind the fins. The streamlines also show that increasing the offset between the fins of the lower and upper walls (*d*=0.6, 1.1, 1.8) widens the fluid passage section, which facilitates the passage of the fluid between the fins in an undulating path, with vortices forming behind the fins.

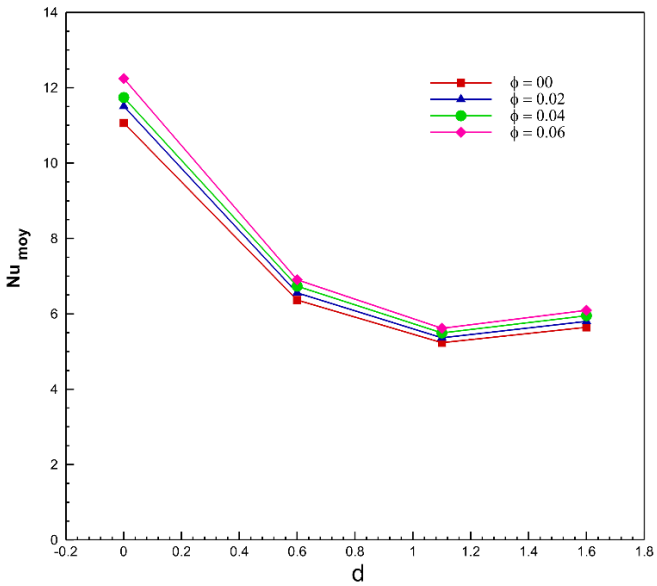

Figure 7. Effect of fin spacing (of hybrid nanofluid) on the Nu_{av} at different concentration values of solid particles, and *Re* =100

The temperature distribution is visualized through the contours of the isotherms, as depicted in Figure 8. The figure reveals a direct correlation between the evolution of the isotherm lines and the distance between the fins on the lower and upper walls (*d*=0, 0.6, 1.1, and 1.6). The correlation is closely linked with the dimensions of the recirculation zone established behind the fins. As the spacing between the fins increases, larger vortices develop, facilitating the transport of a greater amount of heat.

To assess the impact of increasing the fins space of the lower and upper walls, we consult Figure 8 giving the variation in Nu_{av} of the fins for *Re*=100. We can see that Nu_{av} of the fins takes a maximum value for spacing between the fins *d*=0; then decreases to a minimum value with *d*=1.1 and gradually increases again with increased fin spacing. As seen in these figures, increasing or decreasing the spacing between the fins after the value *d*=1.1 increases the heat transfer rate.

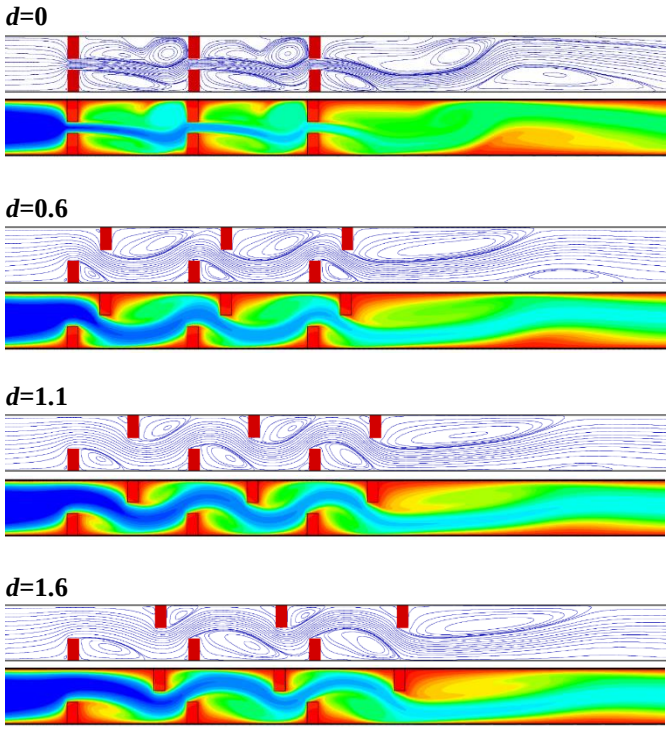

Figure 8. Flow lines (top) and temperature distribution (bottom) for hybrid (ϕ=0.06) nanofluid at different fin spacing "*d*" and *Re*=100

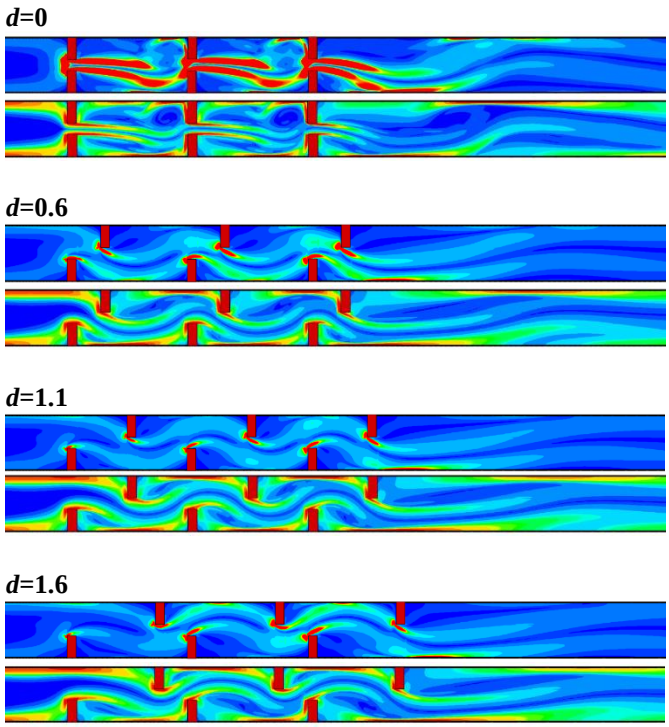

Figure 9. Entropy generation variations due to friction (top) and heat transfer (bottom) for a hybrid nanofluid (ϕ=0.06) at different fin spacing values and *Re*=100

The influence of the spacing between the fins of the upper and lower walls "*d*" on the entropy production contours attributed to friction S_{fr} (top) and heat transfer S_{th} (bottom) inside the channel are presented in Figure 9, for *Re*=100 and ϕ=0.06.

For *d*=0, Figure 9 shows the fluid flow path inside the channel becomes narrower. Also, S_{fr} is very important in a passage located between the fins of the top and bottom walls due to the acceleration of the fluid in this particular zone. With the increase in the spacing between the fins (*d*=0.6, 1.1, 1.6) the intensity of the entropy due to friction decreases and is clustered around the top-left corner of the fins.

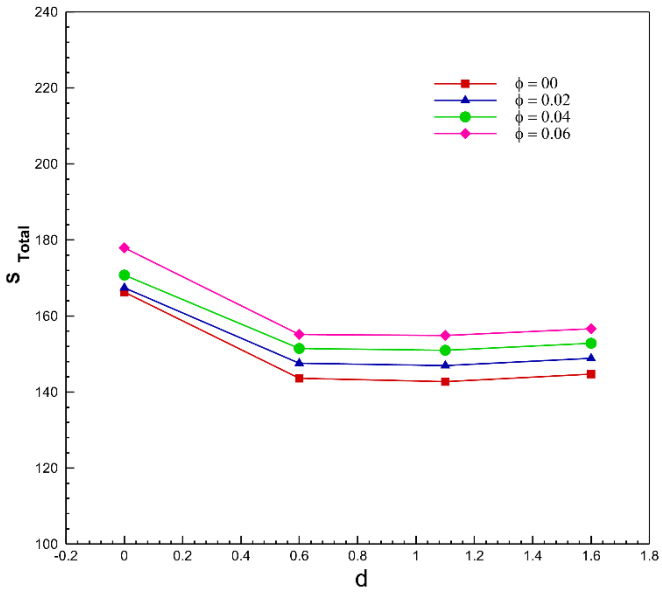

Figure 10. Effects of fin spacing on total entropy generation for various values of ϕ at *Re*=100

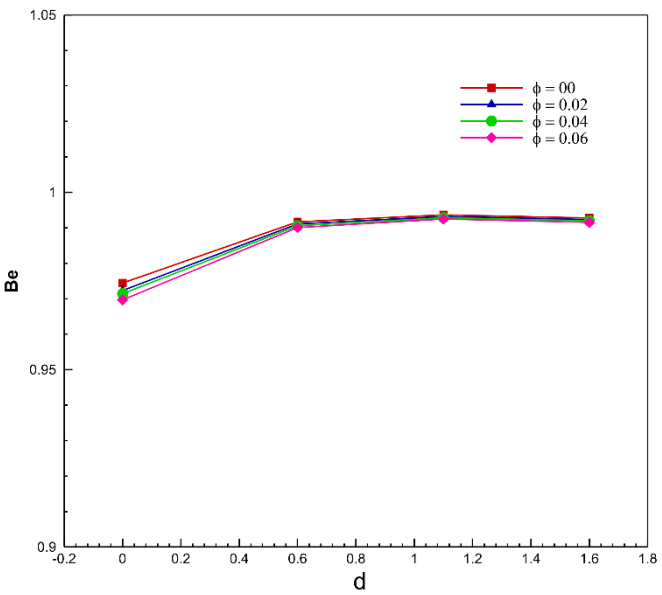

Figure 11. Effects of fin spacing on the Bejan number for various values of ϕ and *Re*= 100

The contours of Entropy generation resulting from heat transfer are also presented in Figure 9. The figure indicates that when *d*= 0, the area near the fins' heated walls and frontal surfaces contains the highest local entropy generation. If the spacing between the fins (*d*=0.6, 1.1, 1.6) increases, the entropy generation contours are concentrated near the upper left corner of the fins and the heated wall.

Figure 10 shows the influence of the space between the fins on S_{total} at *Re*=100 across a range of the concentration of solid particle values. It is evident that S_{total} takes its maximum value for d=0, then a sharp decrease occurs until the value *d*=0.6, and then it increases again slightly until *d*=1.6. The changes in S_{total} are similar for different values of the concentration of solid particles, except that they take on high values for higher values of ϕ.

Figure 11 illustrates the Bejan number's variation for space between the fins "*d*" and the solid volume fraction at *Re*=100. Figure 11 shows that for the different values of ϕ, the Bejan number attains low values for *d*=0, then increases until *d*=1.2, where it slowly decreases. The impact of the ϕ it appears clearly at values of *d*=0, where the increase in ϕ contributes to reducing the *Be* number.

5. CONCLUSIONS

This research conducted a two-dimensional numerical investigation to analyze forced convection in a heated horizontal channel containing fins with hybrid nanofluid Cu-Al_2O_3/water as a cooling fluid. To ensure the results' reliability, a validation of the calculation code was carried out with works already published, and satisfactory agreement was obtained.

The results presented the impact of specific parameters, such as the fin height, the spacing between the fins of the lower and upper walls, and the concentration of solid particles on the flow structure, heat transfer, and entropy production. The previous results lead to the following conclusions:

- Besides improving the heat exchange surface, employing fins enhances heat transfer, particularly with increased fin height. However, it also disrupts fluid flow and raises the total entropy generation concurrently.
- It should be noted that increasing the height of the fins results in a decrease in the Bejan number.
- Expanding the gap between the bottom and top wall fins fosters more flexible fluid passage amidst the fins, which diminishes overall entropy generation. Nonetheless, this alteration also brings about a reduction in heat transfer.
- Increasing the space between the fins "d" leads to an improvement in the Bejan number.
- The utilization of nanofluids has dual effects: it boosts the Nusselt number, thereby enhancing heat transfer; however, it also triggers a simultaneous increase in overall entropy generation.
- The Bejan number becomes minimal for elevated concentrations of solid particles; this appears clearly for high values of "h_f" and low values of "*d*".

REFERENCES

[1] Ghaneifar, M., Raisi1, A., Ali, H.M., Talebizadehsardari, P. (2021). Mixed convection heat transfer of AL_2O_3 nanofuid in a horizontal channel subjected with two heat sources. Journal of Thermal Analysis and Calorimetry, 143: 2761-2774. https://doi.org/10.1007/s10973-020-09887-2

[2] Naderifar, A., Nikian, M., Javaherdeh, K., Borji, M. (2022). Numerical investigation of the effect of fins on heat transfer enhancement of a laminar non-Newtonian

nanofluid flow through a corrugated channel. Journal of Thermal Analysis and Calorimetry, 147: 9779-9791. https://doi.org/10.1007/s10973-022-11222-w

[3] Esfe, M.H., Abbasian Arani, A.A., Azizi T., Mousavi S. H., Wongwises S. (2017). Numerical study of laminar-forced convection of Al_2O_3-water nanofluids between two parallel plates. Journal of Mechanical Science and Technology, 31: 785-796. https://doi.org/10.1007/s12206-017-0130-4

[4] Mehreza, Z., El Cafsib, A. (2021). Forced convection Fe_3O_4/water nanofluid flow through a horizontal channel under the influence of a non-uniform magnetic field. The European Physical Journal Plus, 136: 451. https://doi.org/10.1140/epjp/s13360-021-01410-2

[5] Hannachi, I., Nessab, W., Kahalerras, H. (2023). Variable magnetic field effect on non-Newtonian nanofluid convective flow in a channel containing heated permeable blocks. Arabian Journal for Science and Engineering, 48: 12219-12246. https://doi.org/10.1007/s13369-023-07686-z

[6] Jarray, A., Mehreza, Z., El Cafsi, A.E. (2019). Mixed convection Ag-MgO/water hybrid nanofluid flow in a porous horizontal channel. The European Physical Journal Special Topics, 228: 2677-2693. https://doi.org/10.1140/epjst/e2019-900068-8

[7] Job, V.M., Gunakala, S.R., Gorla, R.S.R., Makinde, O.D., Thameem Basha, H.T. (2023). Unsteady convective ferrohydrodynamic flow of $MnZnFe_2O_4$ /FeCrNbB - EG hybrid nanofluid in a horizontal channel with porous fins and semi-circular heaters. Journal of Magnetism and Magnetic Materials, 571: 170584. https://doi.org/10.1016/j.jmmm.2023.170584

[8] Ltaifa, K.B., D'Orazio, A., Dhahri, H. (2021). Numerical analysis of mixed convection heat transfer and laminar fow in a rectangular inclined micro-channel totally flled with Water/Al_2O_3 Nano fuid. Journal of Thermal Analysis and Calorimetry, 144: 2465-2482. https://doi.org/10.1007/s10973-020-10466-8

[9] Kalteh, M., Abedinzadeh, S.S. (2018). Numerical investigation of MHD nanofluid forced convection in a microchannel using lattice Boltzmann method. Iranian Journal of Science and Technology, Transactions of Mechanical Engineering, 42: 23-34. https://doi.org/10.1007/s40997-017-0073-5

[10] Heidary, H., Hosseini, R., Pirmohammadi, M., Kermani. M.J. (2015). Numerical study of magnetic field effect on nano-fluid forced convection in a channel. Journal of Magnetism and Magnetic Materials, 374: 11-17. http://dx.doi.org/10.1016/j.jmmm.2014.08.001

[11] Alqaed, S., Mustafa, J., Almehmadi, F.A., Sharifpur, M. (2023). Numerical study of entropy generation in the convection heat transfer of nanofluid inside a tilted closed compartment with five constant-temperature heat sources in the presence of a magnetic field. Engineering Analysis with Boundary Elements, 150: 329-341. https://doi.org/10.1016/j.enganabound.2023.02.019

[12] Zamzari, F., Mehrez, Z., Cafsi, A.E., Belghith, A., Quéré, P.L. (2017). Numerical investigation of entropy generation and heat transfer of pulsating flow in a horizontal channel with an open cavity. Journal of Hydrodynamics, 29(4): 632-646. https://doi.org/10.1016/S1001-6058(16)60776-X

[13] Hussain, S., Mehmood, K., Sagheer, M., Ashraf, A. (2019). Mixed convective magnetonanofluid flow over a backwards-facing step and entropy generation using extended Darcy–Brinkman–Forchheimer model. Journal of Thermal Analysis and Calorimetry, 138: 3183-3203. https://doi.org/10.1007/s10973-019-08347-w

[14] Kahalerras, H., Fersadou, B., Nessab, W. (2020). Mixed convection heat transfer and entropy generation analysis of copper–water nanofuid in a vertical channel with non-uniform heating. SN Applied Sciences, 2: 76. https://doi.org/10.1007/s42452-019-1869-2

[15] Kolsi, L., Hussein, A.K., Borjini, M.N., Mohammed, H.A., Aïssia, H.B. (2014). Computational analysis of three-dimensional unsteady natural convection and entropy generation in a cubical enclosure filled with water-Al_2O_3 nanofluid. Arabian Journal for Science and Engineering, 39: 7483-7493. https://doi.org/10.1007/s13369-014-1341-y

[16] Abbaszadeh, M., Ababaei, A., Arani, A.A.A., Sharifabadi, A.A. (2017). MHD forced convection and entropy generation of CuO-water nanofluid in a microchannel considering slip velocity and temperature jump. Journal of the Brazilian Society of Mechanical Sciences and Engineering, 39: 775-790. https://doi.org/10.1007/s40430-016-0578-7

[17] Bhattacharyya, S., Chattopadhyay, H., Swami, A., Uddin, M.K. (2016). Convective heat transfer enhancement and entropy generation of laminar flow of water through a wavy channel. International Journal of Heat and Technology, 34(4): 727-733. https://doi.org/10.18280/ijht.340425

[18] Vatanparast, M.A., Hossainpour, S., Keyhani-Asl, A., Forouzi, S. (2020). Numerical investigation of total entropy generation in a rectangular channel with staggered semi-porous fins. International Communications in Heat and Mass Transfer, 111: 104446. https://doi.org/10.1016/j.icheatmasstransfer.2019.104446

[19] Fersadoua, I., Kahalerras, H., Ganaoui, M.E. (2015). MHD mixed convection and entropy generation of a nanofluid in a vertical porous channel. Computers and Fluids, 121: 164-179. http://dx.doi.org/10.1016/j.compfluid.2015.08.014

[20] Al-Rashed, A.A.A.A., Kolsi. L., Oztop. H.F., Abu-Hamdeh. N., Borjini. M.N. (2017). Natural convection and entropy production in a cubic cavity heated via pin-fins heat sinks. International Journal of Heat and Technology, 35(1): 109-115. https://doi.org/10.18280/ijht.350115

[21] Ghachem, K., Hassen, W., Maatki, C., Kolsi, L., Al-Rashed, A.A.A.A., Borjini, M.N. (2018). Numerical simulation of 3D natural convection and entropy generation in a cubic cavity equipped with an adiabatic baffle. International Journal of Heat and Technology, 36(3): 1047-1054. https://doi.org/10.18280/ijht.360335

[22] Alnaqi, A.A., Aghakhani, S., Pordanjani, A.H., Bakhtiari, R., Asadi, A., Tran, M. (2019). Effects of magnetic field on the convective heat transfer rate and entropy generation of a nanofluid in an inclined square cavity equipped with a conductor fin: Considering the radiation effect. International Journal of Heat and Mass Transfer, 133: 256-267. https://doi.org/10.1016/j.ijheatmasstransfer.2018.12.110

[23] Shahi, M., Mahmoudi, A.H., Raouf, A.H. (2011). Entropy generation due to natural convection cooling of

a nanofluid. International Communications in Heat and Mass Transfer, 38: 972-983. https://doi.org/10.1016/j.icheatmasstransfer.2011.04.008

[24] Ahmed M.A., Alabdaly, I.K., Hatema, S.M., Hussein, M.M. (2023). Numerical investigation of hydrothermal performance and entropy generation through backward facing step channel with oval rib. International Journal of Heat and Technology, 41(5): 1349-1357. https://doi.org/10.18280/ijht.410526

[25] Abu-Nada, E., Masoud, Z., Hijazi, A. (2008). Natural convection heat transfer enhancement in horizontal concentric annuli using nanofluids. International Communications in Heat and Mass Transfer, 35(5): 657-665. https://doi.org/10.1016/j.icheatmasstransfer.2007.11.004

[26] Maxwell, J.C.A. (1881). Treatise Electricity Magn. Second Ed., Clarendon Press, Oxford, UK. https://www.google.dz/books/edition/A_Treatise_on_Electricity_and_Magnetism/A6ENAAAAQAAJ?hl=fr&gbpv=0.

[27] Brinkman, H.C. (1952). The viscosity of concentrated suspensions and solutions. The Journal of Chemical Physics, 20(4): 571. https://doi.org/10.1063/1.1700493

[28] Patankar, S.V. (1980). Numerical heat transfer and fluid flow. Engineering & Technology, Mathematics & Statistics, Boca Raton, 214. https://doi.org/10.1201/9781482234213

[29] Pishkar, I., Ghasemi, B. (2012) Cooling enhancement of two fins in a horizontal channel by nanofluid mixed convection. International Journal of Thermal Sciences, 59: 141-151. https://doi.org/10.1016/j.ijthermalsci.2012.04.015

NOMENCLATURE

Cp	specific heat, $J.kg.K^{-1}$
d	dimensionless separation distance between fins of the lower and upper walls
h_f	dimensionless fin height
H	dimensionless channel height
k*	dimensionless thermal conductivity (k_{fin}/k_f)
Le	dimensionless length of the exit section
Li	dimensionless length of the entry section
L	dimensionless channel length
Nu_{av}	average Nusselt number of fin
P	dimensionless pressure
S	dimensionless separation distance between fins
S_{fr}	dimensionless entropy generation due to viscous friction
S_{th}	dimensionless entropy generation due to heat transfer
S_{total}	dimensionless total entropy generation
T_0	inlet flow temperature, K°
T_h	hot wall temperature, K°
U_0	velocity inlet, $m.s^{-1}$
U, V	dimensionless velocity components
w	dimensionless width of fin
X, Y	dimensionless coordinates

Greek symbols

μ	Dynamic viscosity, Pa.s
ρ	Mass density, kg/m^3
α	thermal diffusivity, $m^2.s^{-1}$ ($k/\rho.Cp$)
β	thermal expansion coefficient, K^{-1}
θ	dimensionless temperature, $(T-T_c)/(T_h-T_c)$
ν^*	dimensionless kinematic viscosities (ν_{fin}/ν_f)
ρ	density, $kg.m^{-3}$
ϕ	solid volume fraction

Subscripts

f	pure fluid
nf	Nanofluid
s	nanoparticle

Non-dimensional Numbers

Be	Bejan number
Ha	Hartmann number
Pr	Prandtl number
Ra	Rayleigh number
Re	Reynolds number